JOM, Vol. 72, No. 2, 2020
https://doi.org/10.1007/s11837-019-03881-2

Chemical Texturization Processes for Non-conventional Silicon Substrates for Silicon Heterojunction Solar Cell Applications

ROCÍO BARRIO ,[1,2] NIEVES GONZALEZ,[1] JULIO CÁRABE,[1] and JOSE JAVIER GANDÍA[1]

1.—Renewable-Energy Department, CIEMAT, Avenida Complutense 40, 28040 Madrid, Spain. 2.—e-mail: rocio.barrio@ciemat.es

The present work addresses the exhaustive study of the surfaces of multicrystalline silicon wafers after being subjected to a texturization process for silicon heterojunction solar cell applications. The investigations described include the effect that the time of isotropic etching based on combinations of hydrofluoric and nitric acids has on the reflectance, the morphology of the surfaces and the surface recombination through the evolution of the implicit open-circuit voltage. The influence of previous treatments and the elimination of porous silicon or silicon oxide formed on wafer surfaces as a consequence of these texturization processes are also addressed. Textured multicrystalline silicon wafer surfaces with a good uniformity and low weighted hemispherical reflectances (23–24%) have been achieved with short etching times. These texturization processes have also been tested on upgraded metallurgical silicon wafers, resulting in weighted hemispherical reflectance values around 23%, but at the cost of the appearance of important surface defects.

INTRODUCTION

Crystalline-silicon photovoltaic (PV) modules today represent about 95% of the global annual market considering both monocrystalline and multicrystalline silicon wafer-based solar cells. These technologies are also expected to play a dominant role during the next decades, owing to their high-yield fabrication process, excellent efficiencies and material abundance.[1] Near-future silicon PV should evolve towards a more sustainable growth with important cost reductions in mass production while maintaining current efficiencies. This could be achieved by developing device structures with low-temperature fabrication processes and with the use of thin wafers or limited-quality silicon absorbers, such as multicrystalline silicon wafers. In this context, silicon heterojunction structures constitute the keystone that allows combining low-temperature processing of thin films and the high efficiency of crystalline silicon.[2,3] In the fabrication of this type of solar cells, the processes for substrate cleaning and surface conditioning (texturization and passivation) are of capital importance. The reason is because of junctions are not formed by the doping part of a solid, as conventional cells based on thermal diffusion, but by growing of silicon thin films onto a silicon wafer.[4] In the case of silicon heterojunction solar cells fabricated with multicrystalline silicon or UMG wafers, usually with a higher concentration of contaminants owing to their particular production method,[5] these stages of their manufacture may be particularly critical.

The light-trapping capacity of solar cells based on silicon wafers can be significantly improved by using textured silicon substrates, owing to the considerable reduction of light reflection they provide with respect to devices based on non-textured wafers. The polycrystalline nature of the substrates considered in this research is not adequate for standard alkaline-based anisotropic etchings (i.e., with NaOH, KOH or Na_2CO_3/$NaHCO_3$ solutions)[6–9] used for monocrystalline silicon wafers, owing to the formation of steps in the crystalline-domain boundaries. In contrast, isotropic etchings based on aqueous solutions of hydrofluoric (HF) and nitric acids (HNO_3) lead to more homogenous surfaces than alkaline solutions.[10–12]

(Published online October 31, 2019)

The present paper describes a systematic and comprehensive study of chemical etching for texturing multicrystalline and limited-quality upgraded metallurgical silicon wafers (UMG-Si), with the goal of attaining surface morphologies that improve optical confinement without inducing defects on the surfaces that become critical interfaces in the fabrication process of silicon heterojunction solar cells. In this regard, special attention has been paid to analyzing the state of these surfaces, which is a critical factor for this kind of cell.

MATERIALS AND METHODS

Characterisation

The spectral hemispherical reflectances [$R_{\mathrm{hem}}(\lambda)$] of the textured silicon surfaces were measured in the spectral range from 300 nm to 1250 nm by means of a UV/Visible/NIR Perkin-Elmer Lambda 1050 spectrophotometer equipped with a 6-nm-diameter integrating sphere at a near angle ($\sim 6°$). The hemispherical reflectance was weighted to the solar spectrum AM1.5G ($G_{\mathrm{AM1.5G}}$) between 350 nm and 1100 nm, given by Eq. 1:

$$R_{\mathrm{hem},w} = \frac{\int_{350}^{1100} R_{\mathrm{hem}}(\lambda) \cdot G_{\mathrm{AM1.5\,G}}(\lambda) \cdot \mathrm{d}\lambda}{\int_{350}^{1100} G_{\mathrm{AM1.5\,G}}(\lambda) \cdot \mathrm{d}\lambda} \qquad (1)$$

The surface morphology of the wafers was analyzed with an optical microscope and a scanning electron microscope (SEM), for which the samples did not require any type of previous preparation because their surface was electrically conductive and unpolished. For each sample, images were taken under both 90° and 45° incidence angles, in the magnification range from × 250 to × 2500 and applying a 20-KV electron accelerating voltage. Energy dispersive x-ray spectroscopy (EDX) was used in conjunction with SEM for the chemical microanalysis of the surfaces in situ. XPS (x-ray photoelectron spectroscopy) was used in order to assess the presence and concentration of chemical impurities after the different texturization processes. The thicknesses of both the porous silicon film and of the silicon-oxide layers grown on the surfaces after texturization, as well as the composition underneath, were obtained by combining XPS and fix-angle sputtering.

The state of surface is extremely important in applications of heterojunction solar cells since the damaged areas and defects can promote the epitaxial growth of the thin amorphous silicon buffer layer, deteriorating its passivation ability.[12] Implicit open-circuit voltages (iV_{oc}) at 1 sun obtained from quasi-steady-state photoconductance (QSS-PC) measurements with a WCT-120 (Sinton Consulting) equipment were used as a measure of the control of the process.[13,14] All the texturization treatments were carried out at room temperatures so that the bulk-carrier recombination was not affected by such processes. Therefore, the variations of iV_{oc} values observed during the texturization processes are only attributed to the surfaces and can be interpreted as the elimination or formation of highly recombinant areas. No passivating layer was deposited onto the surfaces, so very low iV_{oc} values were obtained; thus, their absolute values were not considered. Only variations from sample to sample were used for the analysis, which was focused on assessing the relative evolution of the surface states.[15]

Preparation

The texturization was carried out on both *p*-type as-cut multicrystalline and UMG silicon substrates with resistivities of around 1–2 Ω cm and 200 μm of thickness, respectively. The size of the samples was 40 mm × 40 mm. For chemical texturization, the samples were immersed in an aqueous solution of hydrofluoric and nitric acids (HF:HNO_3:DIW) with a volume ratio 7:1:2 at room temperature. With this composition, with an excess of HF, etching at each point is limited by surface oxidation, which results in uniform morphologies that do not depend on grain orientation. Moreover, lower reflectance ($R_{\mathrm{hem},w}$) values have been achieved in comparison with solutions with excess of HNO_3.[10,16] The etching times were scanned from 30 to 210 s. After the acid etching, all the samples were rinsed two times with de-ionised water (DIW) in order to stop the chemical reaction.

The resulting textured surface is covered by a dark thin film in spite of decreasing reflectance, and increasing recombination making the morphology analysis more difficult. The XPS analysis identifies this film as porous silicon with a thickness between 150 nm and 200 nm. Both the nature and the thickness of such a film are incompatible with our application to heterojunction solar cells, so this film has to be removed. Immersion of the wafers in an aqueous solution of 1% NaOH at room temperature[17] was used for this purpose. The porous silicon etching time was increased from 15 s to 120 s until its total removal was achieved.

RESULTS AND DISCUSSION

Chemical Texturization of Multicrystalline Silicon Wafers

For the acid etching, an HF:HNO_3:DIW solution at room temperature with a volume ratio 7:1:2 was used. Before texturization, $R_{\mathrm{hem},w}$ was 34% on average in the spectral range (350 nm, 1100 nm) (see spectrum (a) in Fig. 1) and the implicit open-circuit voltage only 520 mV. After this chemical texturization process, the resulting surface is covered by a dark thin porous silicon film which brings down the hemispherical reflectance to around 8% on average (see spectrum (b) in Fig. 1). Once this film has been removed, average hemispherical

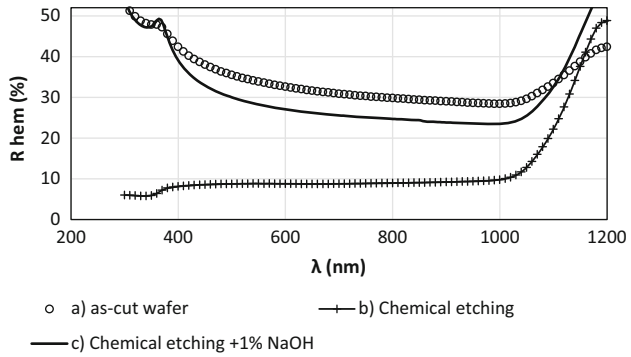

Fig. 1. Spectral hemispherical reflectance in different stages of the acid treatment: (a) as-cut wafer; (b) after treatment with acid solution; (c) after treatment with acid solution and removal of the porous silicon layer with a NaOH solution.

reflectance goes back to values well above 20%, but appreciably below the initial one (see spectra (c) and (d) in Fig. 1).

The acid treatment, after removing the black thin porous silicon layer, produces a uniform textured surface formed by rounded structures like worms or valleys, whose size and aspect ratio depend on the time of treatment. The morphology of the surfaces can be observed on the SEM images in Fig. 2, before and after the texturization treatment. No grain-boundary delineation is observed on the SEM images owing to the isotropic nature of the acid etching. As the etching time progresses, the wafer thickness decreases by some microns, the sizes of the structures increase, and their aspect ratio lowers as they become more rounded. As shown in Fig. 2, acid etching takes too long ($t > 120$ s), and the resulting structures are very large and have low aspect ratios, favoring higher reflectance (see Fig. 3). Too short acid etching times ($t < 90$ s) otherwise produce textured surfaces with deeper features which have lower reflectance, but would be hard to cover by the thin-film emitters required for the fabrication of silicon heterojunction solar cells. Moreover, for short times, the etching depth could not be large enough to eliminate impurities and deteriorated areas of the surfaces. The increase of iV_{oc} with etching time indicates that surface defects of the as-cut wafer are removed in the process. As evidenced by Fig. 3, at a certain etching-time value, iV_{oc} reaches a relative maximum (582 mV for 90-s etching time). Its subsequent decline suggests that, after saw damage has been completely eliminated, additional etching tends to favor surface recombination, maybe as a consequence of an enhancement of chemical reactivity. Therefore, the etching time should be chosen on the basis of a compromise between low hemispherical reflectance and the removal of sufficient saw-damaged material. For these reasons, we propose the range from 90 to 120 s as optimum for this texturization process with $R_{hem,w}$ around 23% on average.

In order to confirm the nature of the porous silicon film generated by the texturization process and to estimate its thickness, the samples were measured by XPS combined with fix-angle sputtering. The thickness of the porous silicon film was between 130 nm and 200 nm. This average thickness has been estimated by XPS depth profiles by taking into account the point at which the ratio of oxygen and silicon concentration is lower than 1 (see an example of depth sputtering in Fig. 4).

Samples with the porous silicon layer removed by a 1% NaOH solution were also analyzed by XPS to determine the presence of surface impurities. Only silicon and oxygen in the form of native oxide (SiO_2) with a thickness around 1–3 nm was present on the textured surface and no other impurity was found (see Table I). Similar results were supported by EDX during the realization of SEM measurements in situ. This native SiO_2 can be removed by immersing the wafers in a 5% aqueous solution of HF at room temperature for 120 s.[18] In view of these results, it can be concluded that acid HF:HNO_3:DIW etching is sufficient for preparing wafer surfaces for silicon heterojunction cell fabrication, not requiring any additional surface cleaning stages.

Furthermore, a previous treatment with NaOH to eliminate saw damage before chemical texturization was also evaluated. This alkaline etching provides surfaces with a polished appearance to the naked eye. The grains are clearly distinguished by their different reflectance with a brilliant aspect. SEM pictures reveal different morphologies according to the orientation of each grain and the presence of steps between grains that sometimes exceed 20 μm in height (see Fig. 5). This morphology is not adequate when depositing a thin amorphous silicon emitter (thickness around 5–10 nm), as required for making silicon heterojunction solar cells.[19] After this treatment, the value of the weighted hemispherical reflectance (350–1100 nm) was between 38 % and 40% on average, depending on the time of the NaOH treatment. Then, these treated wafers were subject to the acid etching described previously (HF:HNO_3:DIW, (7:1:2)). The result was that the acid etching neither softened the steps between grains nor formed an adequate isotropic texturing structure, even for prolonged times. In consequence, the final weighted hemispherical reflectance was around 30%, higher than the same acid treatment without the previous treatment with NaOH.

According to the literature,[20] the acid etching begins in the most deteriorated areas of the surface where atoms are weakly bound to the network and, therefore, are more unstable and reactive. Probably, the NaOH solution tested in this work removes the highly damaged surface of the wafer (more than 10 μm, depending on the time of etching) so that it inhibits the development of the texture derived from the acid etching. This means that the formation of uniformly textured surfaces is very dependent on their initial state and is more favorable toward the surfaces the more deteriorated they are. Consequently, the pre-treatment with NaOH is

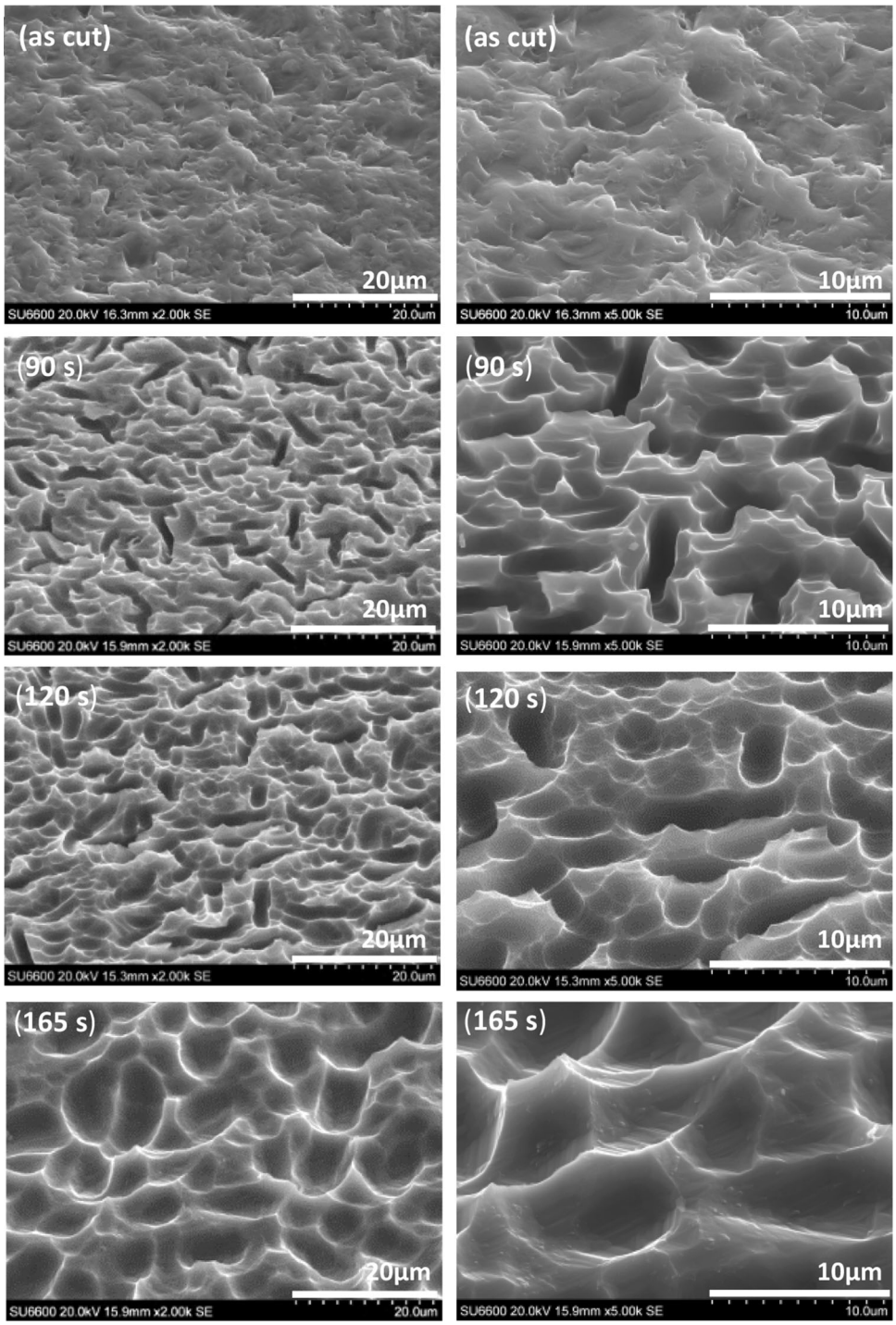

Fig. 2. SEM images of mc-Si wafers before (as-cut) and after texturization processes in which different etching times in acid solution have been applied (90 s, 120 s and 165 s). SEM images have been obtained at, respectively, 45° incidence angle and × 2000 (scale 20 μm) magnification (left column) and 45° incidence angle and × 5000 (scale 10 μm) magnification (right column).

considered unnecessary (even undesirable). In other words, the acid etching is sufficient to remove the most superficial defective layer of the wafer and to form a uniform texture in a single stage.

Chemical Texturization of UMG Wafers

In this research, the etching-based texturing of low-cost UMG substrates was also addressed. Again, in order to reduce reflectance, UMG wafers

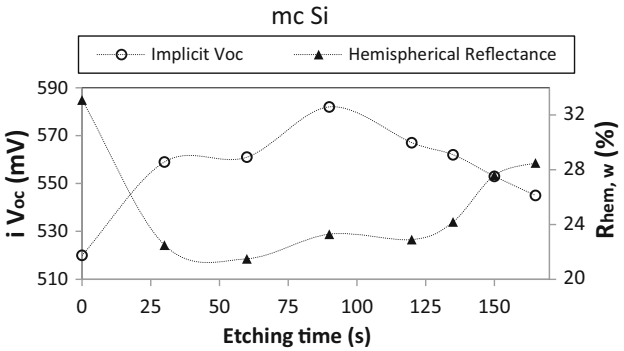

Fig. 3. Evolution of implicit open-circuit voltage (iV_{oc}) and solar-spectrum-weighted average hemispherical reflectance ($R_{hem,w}$) with etching time of mc-Si wafers treated with an HF:HNO_3:DIW (7:1:2) solution. Tests were carried out after removing the porous silicon layer grown during the etching process and without any further passivation.

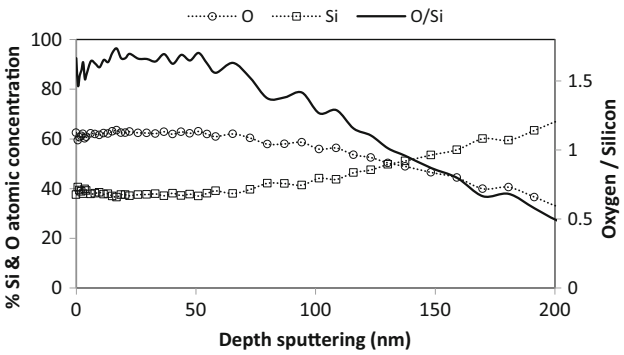

Fig. 4. XPS-depth profile at 45° incidence angle for a multicrystalline silicon wafer after acid treatment. Silicon and oxygen atomic concentrations are normalized to 100%. The thickness of the porous silicon film of this textured sample was estimated to be around 130 nm.

were immersed in the acid texturization solution of HF:HNO_3:DIW (7:1:2) at room temperature, and the time was varied between 60 s and 210 s. Then, the dark porous silicon layer which was formed was eliminated with a 1% aqueous solution of NaOH at room temperature for 120 s. Finally, the samples were rinsed two times in DIW.

As happened with the mc-Si wafers, the acid etching produced a uniformly textured surface with structures whose size increased with treatment duration (Fig. 6). Yet, with UMG wafers subject to large etching times, the development of important surface defects was observed. These defects appear as dark lines along large areas, visible to the naked eye.

The evolution of the weighted hemispherical-reflectance with etching time is not as clear as the one observed for the mc-Si wafers. In Fig. 7, it is possible to appreciate that the reflectance for prolonged times ($t > 135$ s) decreases even though the structures are larger and have a lower aspect ratio. This reduction is attributed to the formation of large grooves and craters. As explained previously, acid etching is more active on deteriorated areas and defects, where the atoms are more unstable and reactive.[20] As a consequence of this, the application of acid etching to UMG wafers discloses the existence of large damaged areas which are not observed on the mc-Si wafers treated under the same conditions. These defects are important recombination centers as can be deduced from the low iV_{oc} values (< 550 mV) that these samples have regardless of the etching time applied (Fig. 7). For this reason, unlike the mcSi wafers, the control of the acid texturization process carried out by the

Table I. Atomic concentrations on the texturized surfaces were analyzed by 45° AR-XPS. The SiO_2 layer thickness has been estimated by XPS depth profiles

	% Atomic concentration		% Si concentration		
Treatment	**O**	**Si**	**SiO_2**	**Si**	**Thickness SiO_2 (nm)**
Texturization	63	37	89	11	~ 207 (porous silicon)
Texturization + 1% NaOH	36	64	13	87	~ 1 (native oxide)
Texturization + 1% NaOH + 5% HF	0	100	0	100	–

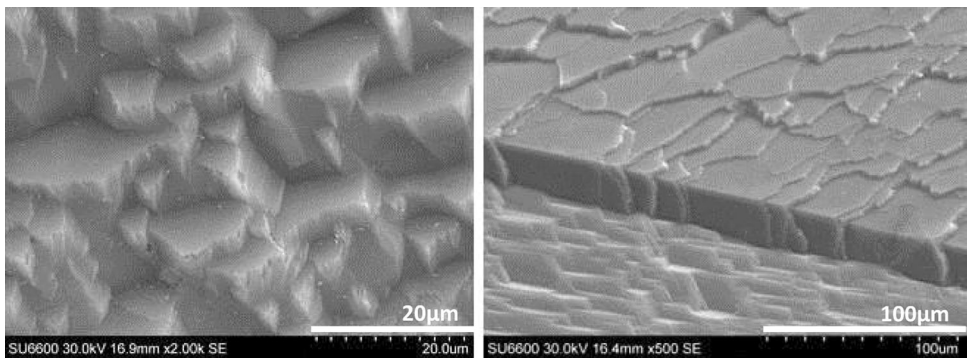

Fig. 5. SEM pictures of mc-Si wafers after 20% NaOH treatment (at 80°C for 10 min). Steps and different morphologies are observed depending on the crystallographic orientation of the grains.

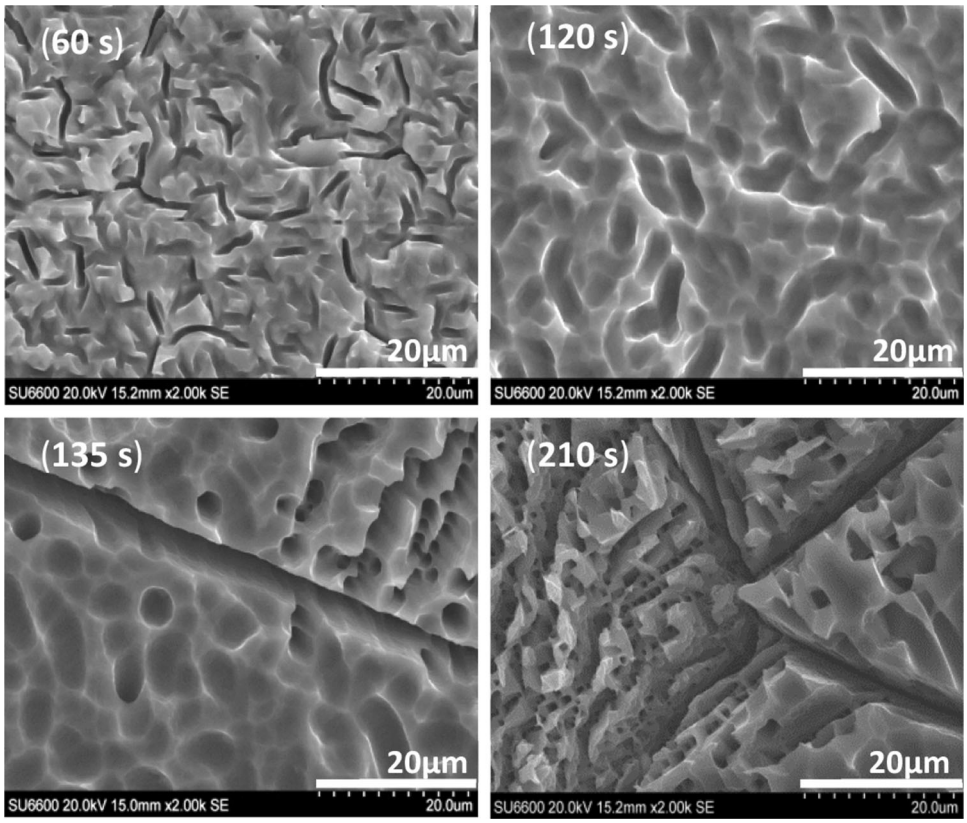

Fig. 6. SEM images of UMG wafers at 90° incidence angle at × 2000 (20 μm) magnification. Samples were textured with a HF:HNO_3:DIW (7:1:2) solution for different etching times (60–210 s). Surface results were very dependent on etching time. For long times, grooves and craters appear on the surfaces.

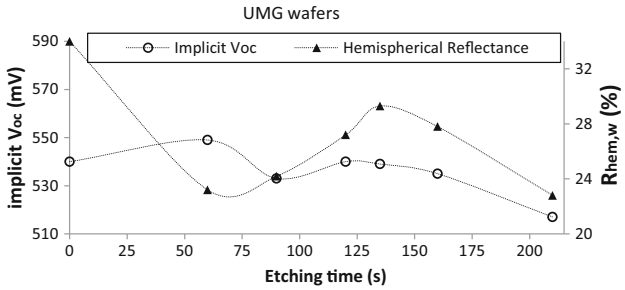

Fig. 7. Evolution of implicit open-circuit voltage (iV_{oc}) and weighted hemispherical-reflectance ($R_{hem,w}$) with HF:HNO_3:DIW (7:1:2) etching time for UMG wafers. The QSS-PC measurements were carried out after the elimination of the porous silicon layer. No surface passivation was carried out.

evolution of the iV_{oc} values is not an adequate method for the UMG wafers. In addition, owing to their morphology and depth, the defects (grooves and craters) could not be easily covered by the passivating films which have to be deposited subsequently. These considerations introduce serious doubts on the suitability of UMG wafers to be used as absorber layers of silicon heterojunction solar cells. However, acid etching should be envisaged as a simple method to detect wafer defects not derived from cutting processes.

CONCLUSION

The texturization of microcrystalline silicon wafers for making silicon heterojunction solar cells has been addressed. A systematic research has been undertaken on a chemical method based on isotropic etching with an aqueous solution of hydrofluoric and nitric acids. The work has allowed not only the reduction of solar-spectrum-weighted average hemispherical reflectances down to 23% but also the simplification of cell fabrication by achieving saw-damage removal and surface texturing in one single step, which requires etching for only between 90 and 120 s. The process includes immersion in an alkaline solution to remove the black porous silicon film generated by acid etching. The control of the process was carried by the evolution of the iV_{oc} values. This simple method allows the assessment of the state of the surface before the application in silicon heterojunction solar cells. Neither impurities nor elements which can be derived from etching were found after this step. Thanks to this, no additional cleaning stages are required.

Although the work has been focused from the beginning on cast multicrystalline silicon, UMG-Si wafers have also been textured. In this case, in spite of reducing the reflectance, the preferential character of the etching has revealed the existence of

important defects which have led to the conclusion both that such wafers are inappropriate for making silicon heterojunction cells and that acid etching can be used as a tool to check surface defects not derived from wafer cutting.

ACKNOWLEDGEMENTS

This work has been partially supported by the Spanish Ministry of Economy and Competitiveness under Project CHENOC (ENE2016-78933-C4-3-R). The authors would like to thank the Unit of Microstructural and Microanalysis Characterization of CIEMAT for SEM and XPS measurements.

REFERENCES

1. I.T. Roadmap, International Technology Roadmap for Photovoltaic (ITRPV) 2014, *Itrpv*. 1. (2015).
2. W. Van Sark, L. Korte, and F. Roca, *Physics and Technology of Amorphous-Crystalline Heterostructure Silicon Solar Cells* (Berlin: Springer, 2012), pp. 1–43.
3. K. Masuko, M. Shigematsu, T. Hashiguchi, D. Fujishima, M. Kai, N. Yoshimura, T. Yamaguchi, Y. Ichihashi, T. Yamanishi, T. Takahama, M. Taguchi, E. Maruyama, and S. Okamoto, *IEEE J. Photovolt.* 4, 6 (2014).
4. M. Taguchii, K. Kawamoto, T. Tsuge, T. Baba, H. Sakata, M. Morizane, K. Uchihashi, N. Nakamura, S. Kiyama, and O. Oota, *Prog. Photovolt. Res. Appl.* 8, 503 (2000).
5. J. Degoulange, C. Trassy, and S. Martinuzzi, *Sol. Energy Mater. Sol. Cells* 92, 1269 (2008). https://doi.org/10.1016/j.solmat.2008.04.020.
6. R. Barrio, N. González, J. Cárabe, and J.J. Gandía, *Sol. Energy* 86, 845 (2012).
7. R. Barrio, N. González, J. Cárabe and J.J. Gandía, *25th European Photovoltaic Solar Energy Conference and Exhibition/5th World Conference on Photovoltaic Energy Conversion*, 6–10 Sept. 2010, Val., Spain.
8. R. Barrio, N. González, J. Cárabe, and J.J. Gandía, *Mater. Sci. Semicond. Process.* 16, 1 (2013).
9. S. Zaynabidinov, R. Aliev, M. Muydinova, and B. Urmanov, *Appl. Sol. Energy* 54, 395 (2018). https://doi.org/10.3103/S0003701X1806018X.
10. K. Kim, S.K. Dhungel, S. Jung, D. Mangalaraj, and J.Ã. Yi, *Sol. Energy Mater. Sol. Cells* 92, 960 (2008). https://doi.org/10.1016/j.solmat.2008.02.036.
11. Y. Cheng, J. Ho, S. Tsai, Z. Ye, W. Lee, D. Hwang, S. Chang, C. Chang, and K.L. Wang, *Sol. Energy* 85, 87 (2011). https://doi.org/10.1016/j.solener.2010.10.020.
12. M. Mews, T. Schulze, N. Mingirulli, and L. Korte, *Energy Procedia* 38, 855 (2013).
13. A. Cuevas and D. Macdonald, *Sol. Energy* 76, 255 (2004). https://doi.org/10.1016/j.solener.2003.07.033.
14. R. Jayakrishnan, S. Gandhi, and P. Suratkar, *Mater. Sci. Semicond. Process.* 14, 223 (2011).
15. P. Drummond, A. Kshirsagar, and J. Ruzyllo, *Solid-State Electron.* 55, 29 (2011).
16. G. Kulesza, P. Panek, and P. Zięba, *Arch. Civ. Mech. Eng.* 14, 595 (2014).
17. E. Stensrud, H. Jorgen, D. Nilsen and A. Holt. *Conference Record of the Thirty-first IEEE Photovoltaic Specialists Conference* (2005). https://doi.org/10.1109/pvsc.2005.1488381.
18. R. Barrio, C. Maffiotte, J.J. Gandía, and J. Cárabe, *J. Non-Cryst. Solids* 352, 945 (2006).
19. A. Ulyashin, M. Scherff, R. Hussein, M. Gao, R. Job, and W.R. Fahrner, *Sol. Energy Mater. Sol. Cells* 74, 195 (2002). https://doi.org/10.1016/S0927-0248(02)00064-8.
20. Z. Xi, D. Yang, W. Dan, C. Jun, X. Li, and D. Que, *Semicond. Sci. Technol.* (2004). https://doi.org/10.1088/0268-1242/19/3/035.